

A THREE-PARAMETER STUDY OF EXTERNAL CAVITY MODES IN SEMICONDUCTOR LASERS WITH OPTICAL FEEDBACK

Vivi Rottschäfer* Bernd Krauskopf**

* *Mathematisch Instituut, Universiteit Leiden, P.O. Box 9512,
2300 RA Leiden, The Netherlands*

** *Department of Engineering Mathematics, University of
Bristol, Bristol BS8 1TR, United Kingdom*

Abstract: An analytical study is presented of the so-called external cavity modes in the Lang-Kobayashi equations, which are a system of delay differential equations that model a semiconductor laser subject to conventional optical feedback. Specifically, the bifurcation set in the space of feedback phase, feedback strength and pump current of the laser is determined. It divides this three-dimensional parameter space into regions with different numbers of physically relevant external cavity modes.

Keywords: Laser with optical feedback, external cavity modes, bifurcation set.

1. INTRODUCTION

A semiconductor laser receiving optical feedback from a conventional mirror is the most basic example of a laser subject to delayed feedback. This system, also called the COF laser, is technologically relevant because in applications, such as optical data storage and optical communication, reflections are often unavoidable. Furthermore, it is known that feedback of less than 1% can already totally destabilize the operation of a semiconductor laser. The laser then typically switches off at irregular intervals; one also speaks of low frequency fluctuations. This is why semiconductor lasers with conventional optical feedback have received a lot of attention, both experimentally and in terms of mathematical modelling; for further information and as general references see the recent surveys Van Tartwijk and Agrawal (1998); Fischer et al. (2000); Gavrielides (2000).

There is a well-established model of the COF laser, the so-called Lang-Kobayashi (LK) equations (first introduced in Lang and Kobayashi (1980)), which, suitably scaled and normalised, can be written as

$$\begin{aligned} \frac{dE}{dt} &= (1 + i\alpha)N(t)E(t) + \kappa e^{-iC_p}E(t - \tau), \\ T \frac{dN}{dt} &= P - N(t) - (1 + 2N(t))|E(t)|^2. \end{aligned} \quad (1)$$

The LK equations (1) are mathematically a system of delay differential equations (DDEs) for the complex electric field $E = E_x + iE_y$ and the inversion (number of electron-hole pairs) N inside the laser. The parameters are the pump current P , the ratio of decay times T , the linewidth-enhancement factor α , the feedback strength κ , the delay time τ , and the feedback phase C_p . We remark that $C_p = \omega_0 \tau$, where ω_0 is the optical frequency. However, for sufficiently large τ the quantity C_p can be seen as an independent parameter; it can be changed, for example, by miniscule changes in the distance of the mirror to the laser (on the order of one optical wave length). In concrete numerical examples we use the parameter values $T = 1710$, $\tau = 70$ and $\alpha = 5.0$ (see Heil et al. (2003)), while C_p , κ and P may vary. Note that for different values of T , τ and α the global picture retains its qualitative features.

In numerous numerical studies the LK equations have been shown to describe experimental observations in

considerable detail when two main modelling assumptions are satisfied, namely, that the feedback is quite weak (on the order of up to a few percent of the emitted light) and that the mirror is quite far away from the laser (on the order of several centimeters to meters).

The topic of this paper is the analytical study of the so-called external cavity modes (ECMs), which are special solutions of Eqs. (1), as a function of the feedback phase C_p , the feedback strength κ and the pump current P . While the potential number of ECMs of a COF laser is known in the literature (see, e.g., Van Tartwijk and Agrawal (1998)), the bifurcation set in the three-dimensional (C_p, κ, P) -space presented here has not been derived before. It divides the (C_p, κ, P) -space into regions with different numbers of physically available ECMs of the COF laser. In this sense this bifurcation set summarizes and extends earlier results in a concise way. Note that here the full DDEs (1) are considered (see also Verduyn Lunel and Krauskopf (2000)); a bifurcation study in the (C_p, κ) -plane for the limit of short delay can be found in Wolfrum and Turaev (2002).

2. THE BASIC SOLUTION

The LK equations (1) have $(E, N) = (0, P)$ as the basic solution, for all choices of the other parameters. When this basic solution is stable the laser is off, and when it is unstable the laser is on. In other words, the bifurcation corresponding to the loss of stability of the basic solution is the laser threshold.

By computing a linear variational equation in the (E, N) -variables around $(0, P)$, its characteristic equation is determined as

$$\left(\lambda + \frac{1}{T}\right) \left[\left(\lambda - P - e^{-\lambda\tau} \kappa \cos(C_p)\right)^2 + \left(\alpha P - e^{-\lambda\tau} \kappa \sin(C_p)\right)^2 \right] = 0. \quad (2)$$

Introducing $\lambda = \nu + i\mu$ in (2), for $\kappa > 0$ and $T > 0$, and splitting the resulting equation into its real and complex parts reveals, after some manipulations, that the basic solution $(0, P)$ undergoes a Hopf bifurcation for

$$C_p^{H\pm}(\kappa, P) = \pm \left[\arccos\left(-\frac{P}{\kappa}\right) + \tau \sqrt{\kappa^2 - P^2} \right] - \alpha\tau P + 2k\pi. \quad (3)$$

Since $C_p^{H\pm}(\kappa, P)$ must be real, a Hopf bifurcation can only take place for $\kappa \geq P$.

Note that $C_p^{H\pm}(\kappa, P)$ forms one smooth two-dimensional surface in (C_p, κ, P) -space (for fixed k). When looking at cross sections for fixed P the resulting curves in the (C_p, κ) -plane change as P is varied. The curves change qualitatively at $P = \frac{1}{\tau}$. In summary, the basic solution $(0, P)$ generally loses its stability at

$P = 0$. However, it is stable in a small closed region for $\kappa > 0$ and $0 < P < \frac{1}{\tau}$; see already Fig. 4.

3. EQUATIONS FOR ECMS

An ECM, sometimes also referred to as a continuous wave solution or CW-state, is a solution with constant intensity and inversion and a phase that depends linearly on time. In other words, it is of the form

$$E(t) = R_s e^{i(\omega_s - \frac{C_p}{\tau})t} \quad \text{and} \quad N(t) = N_s, \quad (4)$$

where R_s , ϕ_s and N_s are constant. Mathematically, an ECM is a periodic orbit in (E, N) -space. It is important to realize that the ECMs are nevertheless the most simple solutions of Eqs. (1) apart from the basic solution, because the LK equations are invariant under the continuous symmetry group of all rotations of the complex E -plane. In fact, each ECM is a group orbit of this continuous symmetry, which means that in projection onto the (R, N) -space it is a single point; see Krauskopf et al. (2000).

In order to find the ECMs one writes Eqs. (1) in polar coordinates by substituting $E(t) = R(t)e^{i\phi(t)}$ and then inserts the ansatz (4). This results in the equations

$$\begin{aligned} 0 &= N_s R_s + \kappa R_s \cos(\omega_s \tau) \\ \omega_s - \frac{C_p}{\tau} &= \alpha N_s - \kappa \sin(\omega_s \tau) \\ 0 &= P - N_s - (1 + 2N_s) R_s^2 \end{aligned} \quad (5)$$

for the constants R_s , N_s and ω_s . Since it is assumed that $R_s \neq 0$, these equations can be simplified to

$$N_s = -\kappa \cos(\omega_s \tau) \quad (6)$$

$$\omega_s - \frac{C_p}{\tau} = -\kappa (\alpha \cos(\omega_s \tau) + \sin(\omega_s \tau)) \quad (7)$$

$$R_s^2 = \frac{P - N_s}{1 + 2N_s} \quad (8)$$

for $N_s \neq -\frac{1}{2}$.

We will use both representations (5) and (7) for ω_s simultaneously. They are transcendental equations and can, therefore, not be solved explicitly for ω_s . However, once ω_s is obtained from (7) (or from (5)), N_s and R_s follow from (6) and (8).

From the way the ECMs are introduced it is clear that R_s must be a *real* constant. Therefore, in order for the solution to be ‘physically relevant’, the condition $R_s^2 > 0$ must hold, which means that from (8) the following restriction on N_s is obtained

$$-\frac{1}{2} < N_s \leq P \quad \text{for} \quad P > -\frac{1}{2}. \quad (9)$$

In section 5 the implication of this restriction will be studied in more detail.

4. THE NUMBER OF POSSIBLE ECMS

The first task is to determine the number of *possible* ECMS irrespective of conditions (9). Equation (7) can be rewritten as

$$\omega_s - \frac{C_p}{\tau} = -\frac{C}{\tau} \sin(\omega_s \tau + \arctan(\alpha)) \quad (10)$$

where $C = \kappa \tau \sqrt{\alpha^2 + 1}$ is called the effective feedback strength. The geometric interpretation is that the ECMS are given as the intersection points of a line and a sine function with amplitude $\frac{C}{\tau}$. Therefore, there is always at least one solution. When κ is increased, the amplitude of the right-hand-side increases and more ECMS are formed in pairs in saddle-node bifurcations.

When defining the functions

$$f(\omega_s) = -\frac{C}{\tau} \sin(\omega_s \tau + \arctan(\alpha)) \quad (11)$$

$$g(\omega_s) = \omega_s - \frac{C_p}{\tau} \quad (12)$$

the intersection points of f and g correspond to ECMS. The saddle-node bifurcation where a new pair of ECMS is formed takes place at exactly those values of κ where $\frac{\partial f}{\partial \omega_s} = \frac{\partial g}{\partial \omega_s}$ and $f = g$. From the first condition, or by differentiating (10) with respect to ω_s , we obtain

$$\cos(\omega_s \tau + \arctan(\alpha)) = -\frac{1}{C} \quad (13)$$

which has solutions as long as $C \geq 1$.

Note that saddle-node bifurcations take place alternately where the function f is positive and negative. For the ECMS formed where $f > 0$ the corresponding N_s is always positive (upon creation) and for the branch where $f < 0$, N_s varies from positive to negative as C_p (or κ) is increased.

It follows from (13) that

$$\sin(\omega_s \tau + \arctan(\alpha)) = \pm \frac{1}{|C|} \sqrt{C^2 - 1} \quad (14)$$

and also that

$$\omega_s \tau + \arctan(\alpha) = \pm \arccos\left(-\frac{1}{C}\right) + 2k\pi \quad (15)$$

for $k \in \mathbf{Z}$, where the sign in Eqs. (14) and (15) is the same. Substituting (14) into (10) and using (15) leads to the expression for the locus of saddle-node bifurcations

$$C_p^{S\pm}(C) = \pm \left[\sqrt{C^2 - 1} + \arccos\left(-\frac{1}{C}\right) \right] - \arctan(\alpha) + 2k\pi. \quad (16)$$

Note that this expression does not depend on the pump P and is 2π -periodic for C_p as was to be expected.

For $C < 1$ no saddle-node bifurcations take place and only one ECM exists. For $C \geq 1$ we can determine the possible number of ECMS in (C_p, κ, P) -space. Since (16) does not depend on the pump current P , intersections with planes $\{P = \text{constant}\}$ all have the same

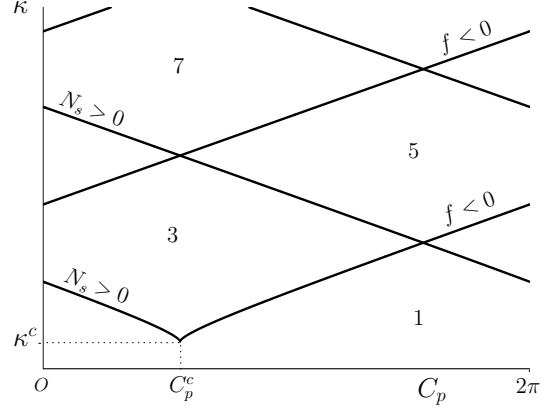


Fig. 1. The number of possible ECMS in the (C_p, κ) -plane; the image is independent of P .

structure that is given in Fig. 1; compare with Van Tartwijk and Agrawal (1998). On these curves in the (C_p, κ) -plane possible ECMS are formed in pairs and we can determine their number in each of the regions separated by the curves. The lowest point of the curves is a cusp point, given by $(\kappa^c, C_p^c) = (1/\tau \sqrt{\alpha^2 + 1}, \pi - \arctan \alpha + 2k\pi)$.

In Fig. 1, we also keep track of whether the ECMS are formed on the saddle-node curve where f is negative or where $N_s > 0$. This is important for the analysis in the next section where we study which of these possible ECMS are physically relevant.

The saddle-node bifurcations take place where (13) holds, which can also be written as

$$\kappa \tau (\alpha \sin(\omega_s \tau) - \cos(\omega_s \tau)) = 1. \quad (17)$$

By substituting (5) and (6) we obtain an expression for the line in the (ω_s, N_s) -plane on which the saddle-node bifurcation takes place, namely

$$N_s = \frac{1 + \tau \alpha (\omega_s - \frac{C_p}{\tau})}{\tau (\alpha^2 + 1)}. \quad (18)$$

Upon substituting the expression for ω_s that was obtained in the above analysis we find the following explicit expressions for N_s and ω_s for the solutions created in the saddle-node bifurcation

$$N_s^S = \frac{1}{\tau (\alpha^2 + 1)} \left[1 \mp \alpha \sqrt{\tau^2 \kappa^2 (\alpha^2 + 1) - 1} \right], \quad (19)$$

$$\omega_s^S = \frac{1}{\tau} \left[C_p \mp \sqrt{\tau^2 \kappa^2 (\alpha^2 + 1) - 1} \right]$$

and R_s can be determined from (8).

The ECMS must also satisfy

$$N_s^2 + \left(\omega_s - \frac{C_p}{\tau} - \alpha N_s \right)^2 = \kappa^2 \quad (20)$$

(by writing (5) as $\omega_s - \frac{C_p}{\tau} - \alpha N_s = -\kappa \sin(\omega_s \tau)$, taking the square of this equation and adding it to the square of (6)). In the (ω_s, N_s) -plane this is an ellipse — the well-known ellipse of ECMS; see, e.g., Van Tartwijk and Agrawal (1998). In Fig. 2 the ellipse

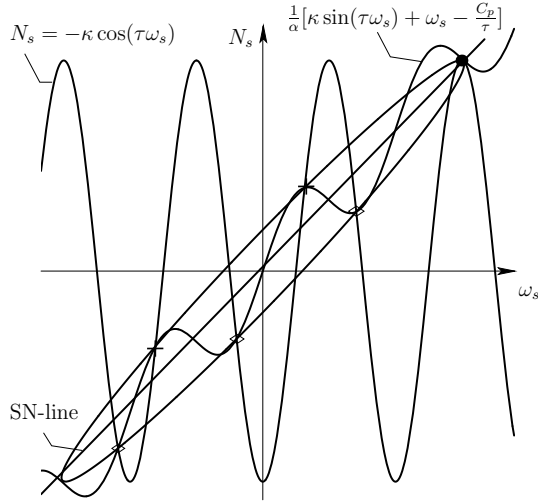


Fig. 2. Plot of the ellipse (20), the graphs of equations (5) and (6), and the line (18) on which the saddle-node bifurcations take place.

(20) is plotted together with the graphs of (5) and (6). Also plotted is the line (18) where the SN-bifurcation takes place (diagonal line). The ECMs are exactly the intersection points of the two graphs of (5) and (6), which indeed lie on the ellipse.

The ECMs above the SN-line are often called ‘anti-modes’. They are marked by the crosses in Fig. 2 and satisfy

$$N_s > \frac{1 + \tau\alpha(\omega_s - \frac{C_p}{\tau})}{\tau(\alpha^2 + 1)}$$

The ECMs below this line are often called ‘modes’; they are marked by the diamonds in Fig. 2.

5. PHYSICALLY RELEVANT ECMS

The possible ECMs that were found in the previous section need to satisfy the two conditions of Eqs. (9), which can be split up into

$$N_s > -\frac{1}{2} \quad (21)$$

$$N_s \leq P. \quad (22)$$

It was noted earlier that ECMs may not be physical for too low pump current; see, e.g., Gavrielides (2000); Haegeman et al. (2002). In this paper it is analyzed what bifurcation occurs in Eqs. (1) when ECMs become (or cease to be) physically relevant.

Conditions (21) and (22) lead to four different regions in the (P, κ) -plane as sketched in Fig. 3. In the region where $\kappa < \frac{1}{2}$ and $\kappa < P$, both conditions are always satisfied. However, in the other regions (21) and (22) are not always automatically satisfied and will lead to extra restrictions as denoted in Fig. 3.

Since κ is assumed to be relatively small, this analysis focuses on the regions below the line $\{\kappa = \frac{1}{2}\}$, specif-

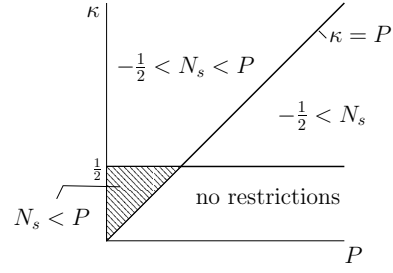


Fig. 3. The different regions in the (P, κ) -plane with the extra restrictions that N_s needs to satisfy in order for R_s to be real.

ically on the shaded region where the extra restriction (22) on N_s needs to be satisfied.

Geometrically, an ECM that moves closer and closer to the boundary where it is no longer physically relevant has a smaller and smaller ‘radius’ R_s . When the boundary is reached, the radius becomes zero, which suggests a Hopf bifurcation with a solution on the axis $\{E = 0\}$ in (E, N) -space. This can only be the basic solution discussed in Sec. 2. Indeed this can be shown analytically as follows.

Substituting $N_s = P$ into equation (6) one obtains the two expressions

$$\omega_s \tau = \pm \arccos\left(-\frac{P}{\kappa}\right) + 2k\pi$$

$$\sin(\omega_s \tau) = \pm \sqrt{1 - \cos^2(\omega_s \tau)} = \pm \frac{1}{\kappa} \sqrt{\kappa^2 - P^2}.$$

Substituting both these equations together with $N_s = P$ into (5) gives the curves where the bifurcation to ECMs with a real amplitude takes place

$$C_p^{P\pm}(\kappa, P) = \pm \left[\arccos\left(-\frac{P}{\kappa}\right) + \tau \sqrt{\kappa^2 - P^2} \right] - \alpha\tau P + 2k\pi, \quad (23)$$

which is indeed exactly expression (3) for a Hopf bifurcation of the basic solution $(0, P)$. In other words, $C_p^{P\pm}(\kappa, P) = C_p^{H\pm}(\kappa, P)$.

The parametrization (23) gives a surface in (C_p, κ, P) -space where $R_s = 0$. When crossing this surface by changing the parameters, ECMs become ‘physically relevant’ (are formed) or disappear. Thus, the sketch of the possible number of ECMs given in Fig. 1 can now be completed to give the actual numbers of physically relevant ECMs. This is shown in Fig. 4 by six representative cross sections given by the (C_p, κ) -plane for fixed P .

The relevant new object is the curve of Hopf bifurcation of the basic solution where physically relevant solutions are born or lost. This curve is tangent to the saddle-node curve at a saddle-node Hopf point (C_p^*, κ^*) , which can be computed as follows. Setting $N_s = P$ in the expression for the N_s -value at the saddle-node bifurcation (19) we find that

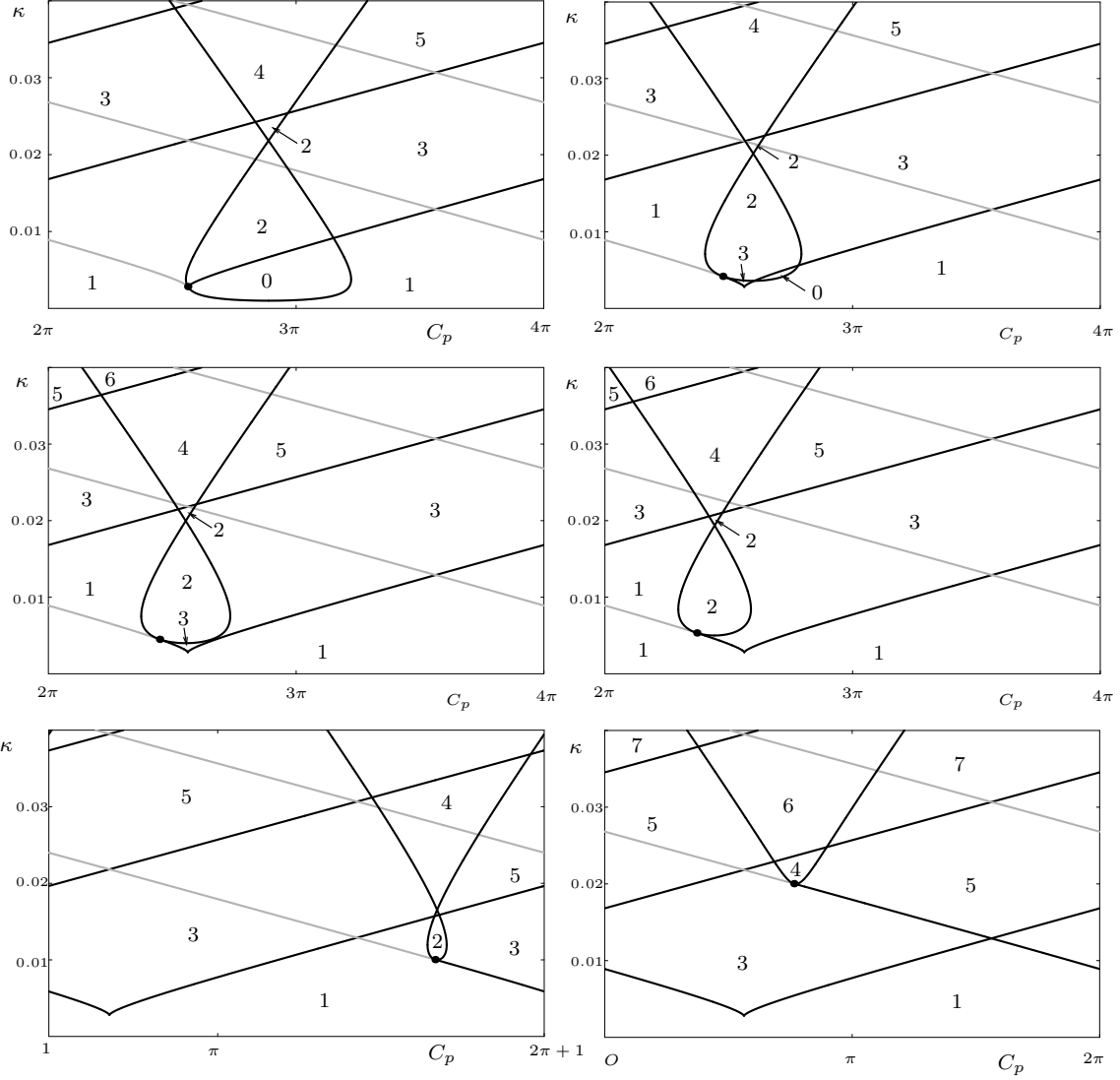


Fig. 4. The bifurcation set in the (C_p, κ) -plane, where from (a) to (f) the pump current P takes the values $P = 0.001$, $P = 0.0036$, $P = 0.004$, $P = 0.005$, $P = 0.01$, and $P = 0.02$. Shown are curves of saddle-node bifurcation and curves of Hopf bifurcation of the basic solution where physically relevant solutions bifurcate. Inside the loop in panels (a) to (e) the basic solution is stable, that is, the laser is off. Along the grey parts of the saddle-node curve the bifurcating ECMs are not physically relevant. Notice that the window of shown C_p values varies from panel to panel to ‘track’ the curve of Hopf bifurcations.

$$\kappa^* = \sqrt{P^2 + \frac{1}{\tau^2 \alpha^2} (1 - \tau P)^2}.$$

The ECMs formed with $N_s > P$ are not physically relevant since they do not satisfy condition (22). The part of the saddle-node curve where this is the case is now plotted in grey; crossing it does not lead to a change in the number of physically relevant ECMs, as can be inferred from the indicated numbers.

The curve of Hopf bifurcation of the basic solution is split by (C_p^*, κ^*) into two parts. For both parts, the number of physically relevant ECMs increases when crossing the curve from left to right. In particular, inside the loop formed by this curve (see Fig. 4(a)–(e)) the basic solution is stable, that is, the laser is off. Physically, this can be interpreted as negative interference (for C_p around π) between the field in

the laser and the reflected field. It appears that there is the possibility of a bistability of this off-state with a stable ECM. However, the full stability analysis of ECMs that would confirm this suggestion is beyond the scope of this paper.

6. FUTURE WORK

The curves in the cross sections of Fig. 4 of saddle-node bifurcations of ECMs and of the Hopf bifurcation of the basic solution form two-dimensional surfaces in the full (C_p, κ, P) -space. They constitute the bifurcation set that bounds the regions with different numbers of physically relevant external cavity modes.

A question that was not addressed here is that of the full stability analysis of the bifurcating ECMs.

For example, it is well known that stable ECMs lose their stability in Hopf bifurcations. We are presently attempting an analytical study of their transcendental characteristic equation. This will allow one to determine the location of further bifurcations, in particular, Hopf bifurcations (including secondary Hopf bifurcations of already unstable ECMs) in an effort to find what one might call the ECM backbone of the system. Knowing this backbone should prove useful for the study of other dynamical phenomena (including periodic and connecting orbits) that can be studied only with advanced numerical techniques, such as numerical continuation and the computation of unstable manifolds.

7. ACKNOWLEDGMENTS

The work of V.R. was supported by the Royal Dutch Academy of Sciences and that of B.K. by an EPSRC Advanced Research Fellowship.

REFERENCES

- I. Fischer, T. Heil, and W. Elsässer. Emission dynamics of semiconductor lasers subject to delayed optical feedback. in *Nonlinear Laser Dynamics: Concepts, Mathematics, Physics, and Applications International Spring School*, edited by B. Krauskopf and D. Lenstra. *AIP Conf. Proc.* **548**, pages 218–237. AIP, Melville, NY, 2000.
- A. Gavrielides. Nonlinear dynamics of semiconductor lasers: theory and experiment. in *Nonlinear Laser Dynamics: Concepts, Mathematics, Physics, and Applications International Spring School*, edited by B. Krauskopf and D. Lenstra. *AIP Conf. Proc.* **548**, pages 191–217. AIP, Melville, NY, 2000.
- B. Haegeman, K. Engelborghs, D. Roose, D. Pieroux, and T. Erneux. Stability and rupture of bifurcation bridges in semiconductor lasers subject to optical feedback. *Phys. Rev. E* **66**:046216, 2002.
- T. Heil, I. Fischer, W. Elsässer, B. Krauskopf, K. Green, and A. Gavrielides. Delay dynamics of semiconductor lasers with short external cavities: bifurcation scenarios and mechanisms. *Phys. Rev. E* **67**(6):066214, 2003.
- B. Krauskopf, G. H. M. Van Tartwijk, and G. R. Gray. Symmetry properties of lasers subject to optical feedback. *Opt. Commun.* **177**:347–353, 2000.
- R. Lang and K. Kobayashi. External optical feedback effects on semiconductor injection laser properties. *IEEE J. Quantum Electron.* **16**:347–355, 1980.
- G.H.M. Van Tartwijk and G.P. Agrawal. Laser instabilities: a modern perspective. *Prog. Quantum Electron.* **22**:43–122, 1998.
- S.M. Verduyn Lunel and B. Krauskopf. The mathematics of delay equations with an application to the Lang-Kobayashi equations. in *Nonlinear Laser Dynamics: Concepts, Mathematics, Physics, and Applications International Spring School*, edited by B. Krauskopf and D. Lenstra. *AIP Conf. Proc.* **548**, pages 66–86. AIP, Melville, NY, 2000.
- M. Wolfrum and D. Turaev. Instabilities of lasers with moderately delayed optical feedback. *Opt. Commun.* **212**:127–138, 2002.